Realisation of a compact laser-pumped Rubidium frequency standard with < $1x10^{-12}$ stability at 1 second

Christoph Affolderbach, Renaud Matthey, Florian Gruet, Thejesh Bandi, Gaetano Mileti

Laboratoire Temps-Fréquence (LTF), Université de Neuchâtel,
Avenue de Bellevaux 51, 2009 Neuchâtel, Switzerland
Email: christoph.affolderbach@unine.ch

INTRODUCTION

We present the realisation and first results of a compact laser-pumped double-resonance Rb frequency standard. The development aims at clock stabilities of $\leq 6x10^{-13}$ at 1 second and $\leq 1x10^{-14}$ at $\tau \geq 10^4$s to one day, in view of applications in, e.g., satellite navigation and space telecommunications.

Implementation of continuous-wave (cw) laser optical pumping in Rb clocks [1] was previously demonstrated to allow excellent short-term clock stability of $3x10^{-13}$ at 1 second [2], and the use of small Rb vapour cells in magnetron-type microwave cavities has resulted in the realisation of highly compact Rb clocks for satellite navigation [3]. In our clock approach, we combine these two technologies in order to realise a compact Rb clock with improved frequency stability, rivalling the stability of much larger and/or more complex clock solutions. In our realised clock prototype the Physics Package occupies a volume of 1.1 litres only and has a mass slightly above 1 kg, including the resonator package and the complete laser optical bench.

Cw laser optical pumping has the advantage of highly efficient optical pumping, which – compared to discharge lamps – results in improved signal contrast and thus improved short-term stability. However, it comes along with more accentuated light-shift effects, which need to be carefully controlled or suppressed in order to achieve the desired long-term clock stability. For this goal, we take advantage of the excellent control of light intensity and frequency possible with laser diodes: The frequency light-shift is controlled by rigorous laser frequency stabilization and the intensity light-shift by control of laser light power and/or fine-tuning the clock cell's buffer-gas content. Instability contributions from the temperature coefficient of the clock cell are reduced by use of a buffer-gas mixture.

In view of long-term operation of a laser-pumped Rb clock over many years, the question of laser diode lifetime is of high importance. In this context, the laser diode lifetime is to be understood as its spectral lifetime, which is the duration during which the laser does not only emit radiation, but also reaches the precise wavelength of the Rb transitions. We have started a dedicated experiment to study this question for the laser diodes used in our Rb clock, by long-term measurements foreseen to run over several months.

CLOCK REALISATION

The clock scheme is based on the laser-pumped double-resonance Rb clock approach reported previously [1, 4]. We use a DFB laser diode emitting at 780nm (Rb D2 line) for optical pumping of the atoms. The laser housing includes a thermoelectric cooler and is integrated on a sub-mount together with the laser collimator and an optical isolator. We measure the laser intensity noise (RIN) and frequency noise to be $5x10^{-14}$ Hz^{-1} and 6 $kHz/Hz^{1/2}$, respectively, both at the clock modulation frequency around 300 Hz. The laser linewidth is < 4 MHz, sufficient to resolve sub-Doppler resonances from a simple saturated-absorption setup. Laser frequency stabilisation to these reference lines is achieved by frequency modulation of the laser light and lock-in detection. All laser control electronics is standard LTF custom-made electronics.

The laser light optically pumps ^{87}Rb atoms contained in the clock cell (volume 2.4 cm^3), that also contains a buffer gas for line narrowing. All Rb cells used (clock cells and laser reference cell) are produced in our LTF facilities. The cell is placed in a magnetron-type microwave resonator with TE_{011}-like mode structure that allows for reduced resonator size [5]. Microwave radiation at 6.8 GHz produced by a low phase-noise synthesizer is directly injected into to the

microwave resonator. The resonator is equipped with a thermostat heater and c-field coils, and is surrounded by a three-layer magnetic shield. The c-field current and thermostat loop are provided by LTF custom-made electronics (relative current stability of 2×10^{-6} at 1 day, thermostat stability ≈ 50μK at 1 day). The clock signal is detected in the light intensity transmitted through the cell, focussed onto photodetectors placed outside the magnetic shields.

Fig. 1 shows the CAD design and a photograph of the clock demonstrator Physics Package. A common, thermostated baseplate carries the laser source and the laser reference cell assembly (seen on the left-hand side in Fig. 1) and two clock resonator assemblies (rectangular magnetic shields on the right-hand side in Fig. 1). Two clock resonator assemblies with identical Rb cells are implemented for noise cancellation [2]. The miniature optical breadboard between the two parts serves for beam alignment and light intensity adjustment. The overall volume of the clock demonstrator is 2.4 litres (240mm x 100mm x 100mm), of which only 1.1 litres are occupied by the complete optical bench and clock resonator packages.

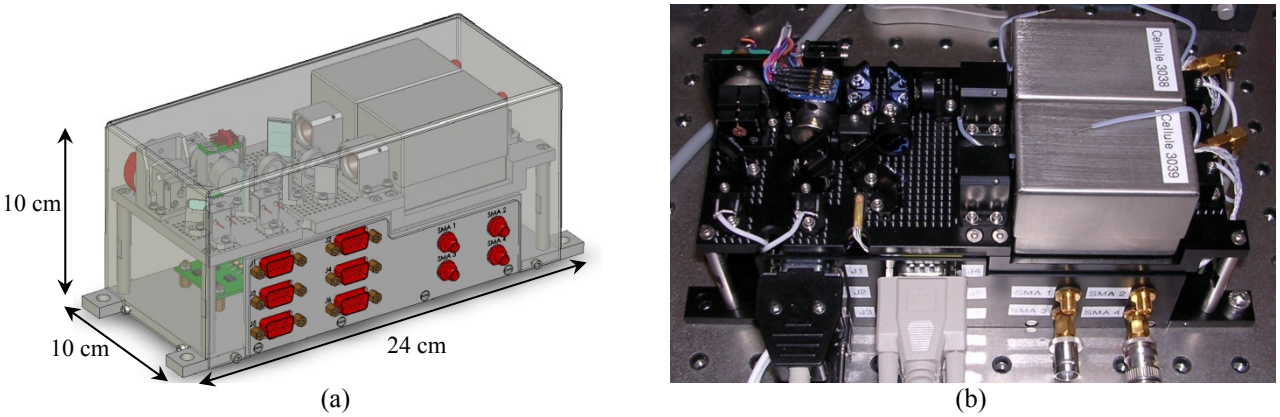

Figure 1 : (a) CAD outline and (b) photograph of the assembled clock demonstrator.

Short-term stability

Figure 2a gives a typical clock signal for the m_F=0→0 clock transition, having a linewidth of 660Hz and a contrast of 10%. By implementing a square-wave modulation to the microwave synthesizer and subsequent lock-in detection we derive an error signal with a discriminator slope of $D \approx 600$ pA/Hz. From measured detection noise N and the formula given in [6], we derive the signal-to-noise limit for the short-term stability as:

$$\sigma_y(\tau) = \frac{N}{\sqrt{2}\cdot D\cdot f_0}\cdot\tau^{-1/2} \approx 8.7\times10^{-13}\,\tau^{-1/2} \qquad (1)$$

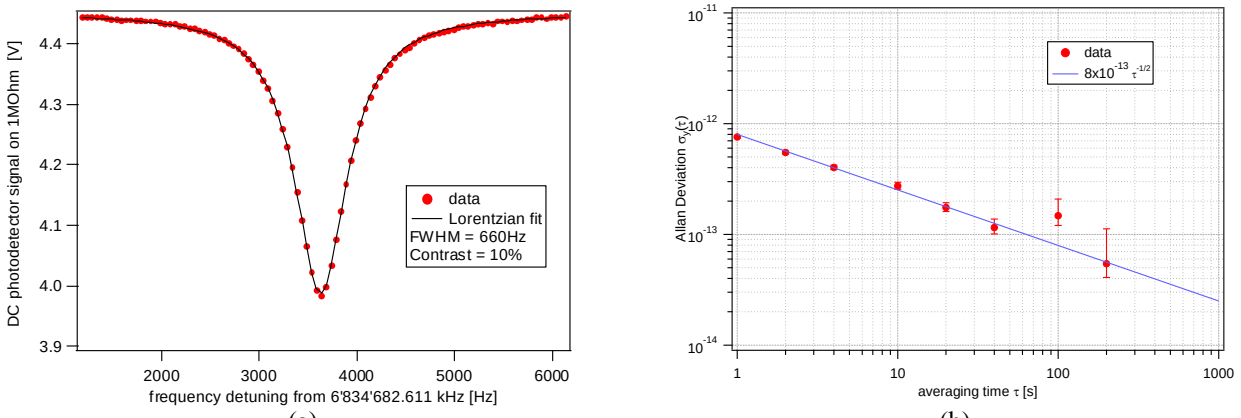

Figure 2 : (a) example of clock signal and (b) measured short-term clock stability.

The experimentally measured short-term stability of the clock is shown in Figure 2b and follows $8x10^{-13}\ \tau^{-1/2}$. This value is in good agreement with the calculated S/N-limit. Table 1 gives an overview on the contributions to the clock's short-term stability stemming from different sources. The shot-noise limit of the clock is $2x10^{-13}\ \tau^{-1/2}$ and the main contribution to the overall clock instability currently is due to laser noise (including AM-FM noise conversion in the clock cell). It is foreseen to further reduce this latter instability contribution by noise cancellation (using the second clock cell in the demonstrator PP) and/or improved laser stabilisation [2]. Such reduction of the laser noise by a factor of two will allow reaching a short-term stability of $< 6x10^{-13}\ \tau^{-1/2}$.

Table 1 : Contributions of the different sources to the clock's short-term instability.

Source	**Instability contribution**
Shot-noise limit	$2.0x10^{-13}\ \tau^{-1/2}$
Microwave noise (synthesizer + loop)	$3.6x10^{-13}\ \tau^{-1/2}$
Laser noise (without noise cancellation)	$7.7x10^{-13}\ \tau^{-1/2}$
Total S/N limit	$8.6x10^{-13}\ \tau^{-1/2}$
Line shifts (Light-shift)	$1.1x10^{-13}\ \tau^{-1/2}$
Total stability prediction	$8.7(5)x10^{-13}\ \tau^{-1/2}$

Parameter optimisation for medium-term stability

In view of well-controlled medium-term clock stability, the relevant parameters such as light-shift parameters, laser frequency stability, and the temperature coefficient (TC) of the clock cell have been evaluated. These parameters were measured (as described below) and their contributions to the clock instability are summarized in Table 2. The total stability prediction is $4.7x10^{-15}$ at $\tau \geq 10^4$s, compatible with a clock stability of $\leq 1x10^{-14}$ at several hours up to 1 day of integration time. Cavity pulling gives a negligible contribution due to the low resonator Q-factor ≈ 240 and cavity tuning of < 100 kHz/K. The microwave power shift might give an additional instability contribution on the level of $1x10^{-14}$ (under evaluation).

Table 2 : Predicted level of clock instability contributions from different effects, calculated from measured parameters. The implemented means of controlling the different effects are also mentioned.

Effect	**Controlled by**	**Instability contribution at $\tau \geq 10^4$s**
Frequency light shift	Laser stabilisation to saturated absorption lines from a separate reference cell	$4x10^{-15}$
Intensity light shift	Pump-light frequency detuning (adjustment of total buffer-gas pressure)	$6x10^{-16}$
Temperature coefficient	Adjustment of buffer-gas mixture	$1x10^{-15}$
Second-order Zeeman shift	C-field current	$2x10^{-15}$
Cavity pulling	Cavity temperature	$< 1x10^{-16}$
Total stability prediction		$4.7x10^{-15}$

Laser Frequency Stabilisation

Narrow sub-Doppler resonances for laser frequency stabilisation are obtained from a small separate Rb vapour cell using a simple, retro-reflected saturated absorption setup without subtraction of the Doppler background. In a previous version of our frequency-stabilised laser head, the achieved frequency stability was partly limited by fluctuations in cell temperature and magnetic field [7]. We have therefore realized a new reference cell assembly (Fig. 3a) that includes: a small Rb vapour cell (9mm diameter x 19mm length); thermostat heater elements at the cell windows; two layers of magnetic shields. The complete reference assembly occupies a volume of < $(30mm)^3$. Fig. 3b gives the frequency stability of the laser stabilised to this assembly, obtained by a beat measurement between two identical laser heads equipped with the new cells. At $\tau \geq 10^4$s the frequency stability is improved by almost one order of magnitude, and reaches $3x10^{-13}$, i.e., ≈ 100 Hz at the optical frequency. It thus fulfils the stability specifications for the clock.

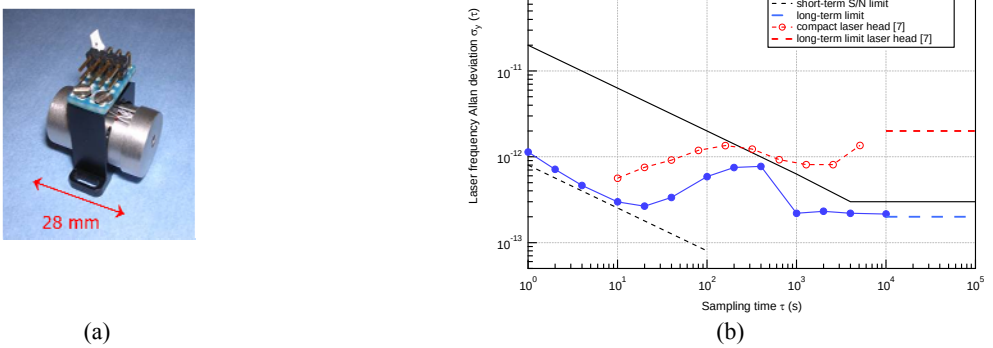

(a) (b)

Figure 3 : (a) Fully mounted reference cell assembly. (b) Frequency stability of the laser head updated with the new reference cell assembly. The frequency stability is improved by one order of magnitude compared to the data and long-term limit reported for a previous version of the compact laser head [7].

Intensity Light-Shift

Minimized intensity light-shift is obtained when the pump laser frequency is tuned close to the centre of the optical transition that is broadened by the buffer-gas in the clock cell. With the laser frequency stabilised to the given Rb saturated absorption lines in the separate laser reference cell, we adjust the optical transition in the clock cell to the laser frequency by exploiting the frequency shift of the optical line as a function of buffer-gas pressure [8]. By adjusting the total buffer-gas pressure filled into the clock cell to within fractions of a millibar, we achieve an intensity light-shift coefficient of $\alpha = 4x10^{-14}$ $cm^2/\mu W$ (Fig. 4). This low value results in only week requirements on the intensity stability of the pump-light, making it possible to run the clock with the inherent intensity stability of the frequency-stabilised laser.

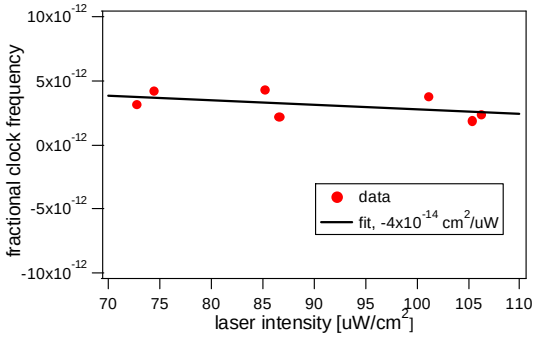

Figure 4 : Measured intensity light-shift for a cell with optimized total buffer-gas pressure.

Temperature Coefficient of the Clock Cell

Pure buffer gases added to the clock cell result in a temperature shift of the clock transition of typically 10^{-9}/K [9], too large for the clock stability envisaged here. By choosing the correct mixture of two gases with opposite temperature shift (Ar + N2 here), the first-order shift cancels and a quadratic behaviour remains (Fig. 5b). The turning point of the parabola then gives the operating temperature for minimal temperature coefficient, ≈ $1x10^{-11}$/K around T_{cell} ≈ 53°C in this case. For these measurements, we correct for light-shift of the clock frequency by locking the laser to different reference lines, and extrapolate to zero intensity light-shift for each laser frequency (Fig 5a). Because the light shift is linear with laser frequency and intensity here, the crossing point of the fit lines gives the clock resonance frequency under condition of zero light-shift, making the temperature shift the dominant effect.

We have also studied the repeatability of the cells' temperature coefficient, by repeating the identical cell filling procedure for four independent runs of cells, distributed over 3 months. The gas mixture is prepared each time starting from laboratory-grade pure gases. For all cell runs, we find the turning point of the parabola to lie between 53°C and 58°C, which indicates good reproducibility of the process.

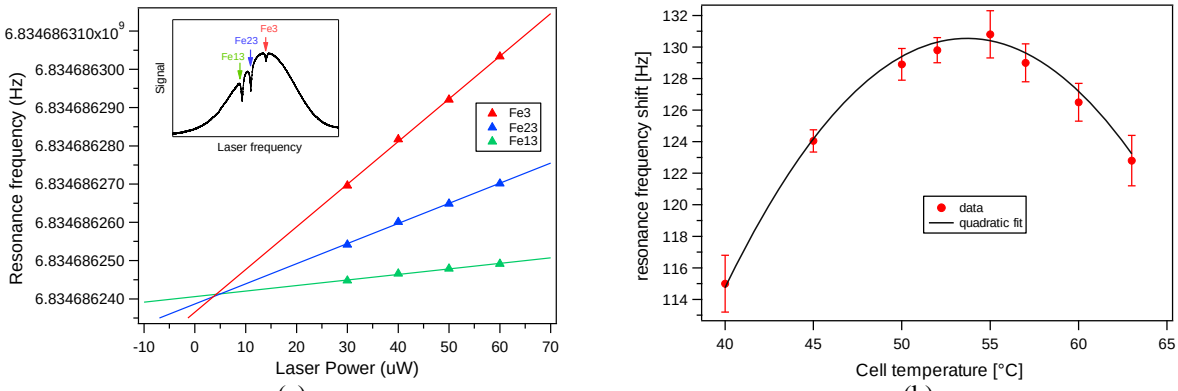

Figure 5 : (a) Method for extrapolation to zero light-shift. The inset indicates the laser locking positions used on the F_g=2 component. (b) Temperature coefficient of the cell (same cell as for Fig. 4).

LONG-TERM STUDIES

Laser Spectral Aging Studies

There is presently a lack of information and background concerning the aging of laser diodes, in particular of their spectral properties. This element is however of paramount importance in view of their application in any kind of future atomic clocks. In such clocks, the laser diode is usually locked to a given atomic transition or spectral feature (e.g. cross-overs in saturated absorption spectroscopy set-up). Due to its influence on the overall clock frequency stability, the stability of the laser injection current (for a given constant temperature) at the locking point must be inquired.

To help gathering knowledge on this subject, we have assembled a laser diode spectral aging system. It allows measuring laser diode parameters like laser threshold current, frequency and optical power tuning rates with laser current and temperature, atomic resonance reachability, current at resonance for a constant temperature, and, using additional laboratory instruments, relative intensity noise (RIN), frequency noise, laser linewidth. By current at resonance, we here mean the injection current for the laser diode to emit a precise optical frequency, which corresponds to some atomic resonance in the application we are interest in.

As illustrated in Fig. 6(a), the system consists mainly of *i*) a computer-driven platform that controls the temperature and injection current of laser diodes and records signals from photodetectors and of *ii*) an optical setup including a frequency discriminator (Rb87 vapour gas cell) for the characterization of a variety of laser diodes (DFB lasers, VCSEL's, Fabry-Perot or similar lasers) mounted in various housings (with and without integrated thermoelectrical cooler TEC device, TO-3, TO 5.6-mm, TO 9-mm packages) and emitting at D1 or D2 Rb resonance wavelength. The optical setup provides a fibre-connected output for additional measurements with other optical instrumentation. By

changing the frequency discriminator (here the atomic vapour cell), laser diodes emitting at other wavelengths can be tested (e.g. Cs D1 and D2). One or two laser diodes can be implemented and tested in the present set-up; yet, it was conceived to be extended to more devices.

The laser parameters (temperature, current, voltage) and the photodetector signals are recorded in data files for further analysis. Ramp measurements by ramping either the diode current or temperature can be realised once only or automatically repeated at regular time interval to evaluate the laser diode behaviour with the time (aging). A fixed laser diode temperature and current applied between two successive measurements can be chosen independently from the values applied during ramp measurements, for thermal cycles and accelerated aging tests. The highest applicable temperatures are imposed by the power of the Peltier devices integrated in the laser diode housing or laser diode mount.

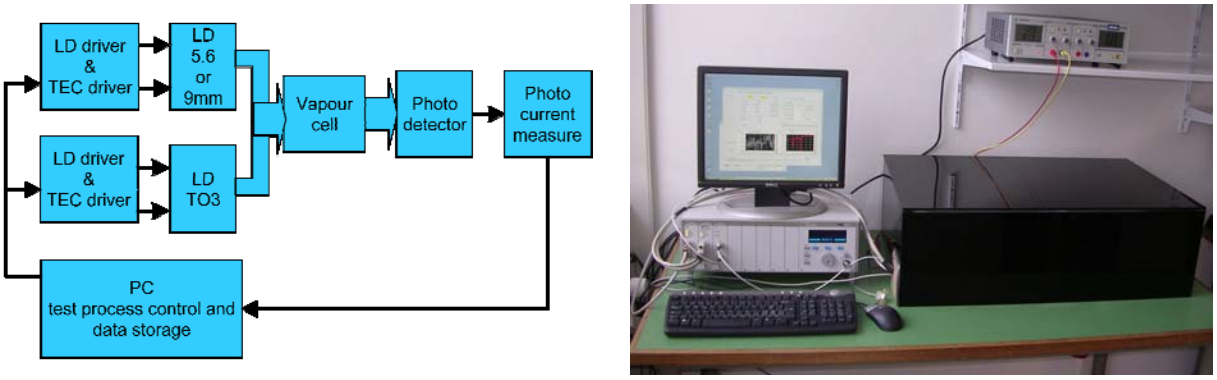

(a) (b)

Figure 6 : (a) Laser diode aging system approach. (b) View of the system as installed in a laboratory room. The dark plastic box on the right contains the optical setup.

During several weeks, the aging system has successfully performed uninterrupted automated measurements of two DFB lasers at 780 nm, one in a TO-3 package with integrated TEC, the other in a TO 9-mm package. The evolution of the current at resonance for the laser diode with integrated TEC is shown as example in Fig. 7. This parameter is the current at which the ^{87}Rb (F=2) is reached for a temperature of 26.5°C. It is retrieved from measurements realised each 3 hours by a current ramp scanning the resonance. Between two successive measurements, the laser is maintained in operation at the same temperature and at 108 mA. As determined from continuous records of the outside temperature and the temperature inside the protection box, the fluctuations reflect the laboratory room temperature variations (day/night alternation). The daily fluctuations correspond to 0.1% of the current value. Several additional weeks of measurements will yield first hints on the behaviour of the laser diode.

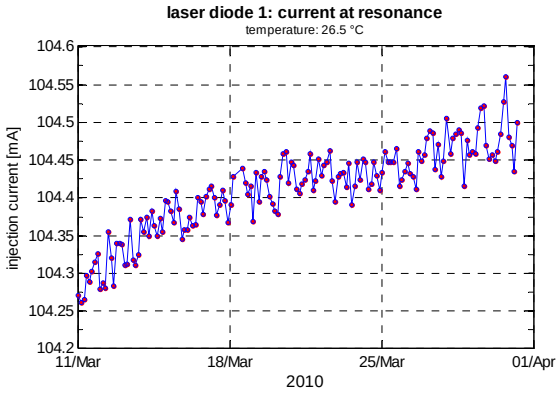

Figure 7 : Time evolution of the current at resonance for the laser diode with integrated Peltier element. The current variations are caused by actual ambient lab temperature fluctuations; they are not due to system noises.

Long-Term Studies of a Laser-Pumped Rb Clock

In order to investigate on the long-term stability performance of a laser-pumped Rb clock, we have set up a clock system similar to the one described in [4] to operate inside a vacuum chamber. This clock is based on a modified Galileo RAFS module [3], optically pumped by a compact laser head as described in [7] but employing a DFB laser diode. The clock successfully operates under vacuum (10^{-6} mbar level) and the system includes monitoring of key parameters of the laser and RAFS module. The clock stability (see Fig. 8) is $1.4\times10^{-12}\ \tau^{-1/2}$ up to 20 seconds and reaches the 1×10^{-13} level at $\tau > 2\times10^{4}$s, which is sufficient to detect certain frequency instabilities reported for lamp-pumped clocks [10]. By acquiring sufficiently long records of data, this study will contribute to identify the origin of these instabilities, and help answering if similar instabilities also occur in a laser-pumped Rb clocks.

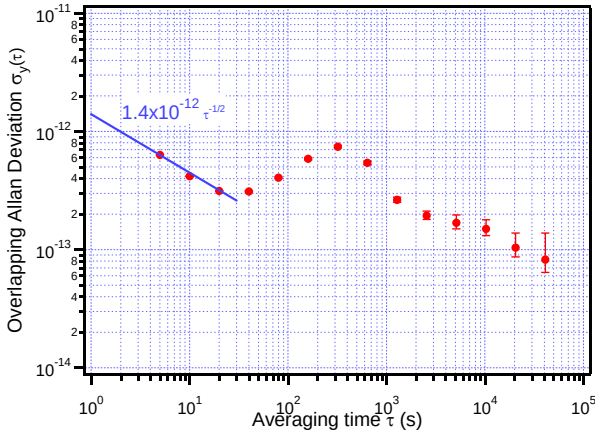

Figure 8 : Frequency stability of a laser-pumped Rb clock based on a modified Galileo RAFS module and a DFB laser head, operating under vacuum. The stability reaches 1×10^{-13} level at 20'000s, sufficient for the envisaged studies.

CONCLUSIONS

We have demonstrated a laser-optically pumped Rb clock with a short-term stability of $8\times10^{-13}\ \tau^{-1/2}$, using a simple cw pumping scheme. Further improvement towards the shot-noise limit of $2\times10^{-13}\ \tau^{-1/2}$ is expected from implementation of laser noise cancellation schemes, without need for pulsed operation or cold atoms. The main effects limiting the one-day stability of the clock, such as light shifts and clock cell temperature coefficient, are controlled and contribute < 5×10^{-15} to the clock stability at one day. A compact clock demonstrator Physics Package was realised that contains the full clock physics including the complete laser optical bench within 1.1 litres of volume. Work is in progress to demonstrate the expected long-term stability with this clock demonstrator.

In view of laser-pumped atomic clocks deployed for long-term applications, the impact of the laser source aging on its spectral behaviour must be studied. Although of interest, such studies are very scarce. To this aim, we have assembled a laser diode aging system. The system is now running and two DFB laser diodes are under tests. First evaluation results are expected in the next months.

ACKNOWLEDGMENTS

We acknowledge financial support by the European Space Agency (ESTEC contract 19392/05/NL/CP), the Swiss Space Office, Fondation en faveur d'un Laboratoire de Recherche Horlogère, Swiss National Science Foundation (grant 200020-105624), and Université de Neuchâtel. We thank our colleagues D. Miletic, M. Pellaton, P. Scherler, and M. Durrenberger (all at LTF-UniNe) for experimental assistance and their contributions to the realisation of the hardware. We thank A. Skrivervik and F. Merli (both at EPFL-LEMA) and H. Schweda for their inputs on the realisation of the microwave resonator, F. Ascarrunz (SpectraDynamics Inc.) and C. Calosso (INRIM) for help with the microwave synthesizers, and Spectratime SA for support with the RAFS tests and monitoring.

REFERENCES

[1] J. Vanier, C. Mandache, "The passive optically pumped Rb frequency standard: the laser approach", Appl. Phys. B, vol. 87, pp. 565-593, May 2007.

[2] G. Mileti, J. Deng, F. L. Walls, D. A. Jennings, R. E. Drullinger, "Laser-Pumped Rubidium Frequency Standards: New Analysis and Progress", *J. Quantum Electronics*, Vol. 34, pp. 233-237, February 1998.

[3] F. Droz et al., "On-Board Galileo RAFS, current status and performances", *Proceedings of the 2003 IEEE International Frequency Control Symposium Jointly with the 17th European Frequency and Time Forum*, pp. 105-108, 2003.

[4] C. Affolderbach, F. Droz, G. Mileti, "Experimental Demonstration of a Compact and High-Performance Laser-Pumped Rubidium Gas Cell Atomic Frequency Standard, *IEEE Trans. Instrum. Meas.*, vol. 55, pp. 429-435, April 2006.

[5] G. Mileti, I. Rüedi and H. Schweda, "Line inhomogeneity effects and power shift in miniaturized rubidium frequency standards", *Proc. 6th EFTF*, pp. 515-519, March 1992.

[6] G. Mileti, P. Thomann, "Study of the S/N Performance of Passive Atomic Clocks Using a Laser Pumped Vapour", *Proceedings of the 9th European Frequency and Time Forum*, Besançon, pp. 271-276, 1995.

[7] C. Affolderbach, G. Mileti, "A compact laser head with high-frequency stability for Rb atomic clocks and optical instrumentation", *Rev. Sci. Instrum.* vol.76, 073108, 2005.

[8] M. D. Rotondaro, G. P. Perram, " Collisional broadening and shift of the rubidium d_1 and d_2 lines (5^2S_{12} -> 5^2P_{12}, 5^2P_{32}) by rare gases, H_2, D_2, N_2, CH_4 and CF_4", *J. Quant. Spectrosc. Radiat. Transfer*, vol. 57, pp. 497-507, April 1997.

[9] J. Vanier, R. Kunski, N. Cyr, J. Y. Savard, M. Têtu, "On hyperfine frequency shifts caused by buffer gases: Application to the optically pumped passive rubidium frequency standard", *J. Appl. Phys.*, vol. 53, pp. 5387-5391, August 1982.

[10] J. C. Camparo, C. M. Klimcak, S. J. Herbulock, "Frequency Equilibration in the Vapour-Cell Atomic Clock", *IEEE Trans. Instrum. Meas.*, vol. 54, pp. 1873-1880, October 2005.